Enzyme Models

DOI: 10.1002/anie.201404133

Hexacoordinate Nickel(II)/(III) Complexes that Mimic the Catalytic Cycle of Nickel Superoxide Dismutase**

*Sudip K. Chatterjee, Ram Chandra Maji, Suman Kumar Barman, Marilyn M. Olmstead, and Apurba K. Patra**

Dedicated to Professor Pradip K. Mascharak

Abstract: *A functional model complex of nickel superoxide dismutase (NiSOD) with a non-peptide ligand which mimics the full catalytic cycle of NiSOD is unknown. Similarly, it has not been fully elucidated whether NiSOD activity is a result of an outer- or inner-sphere electron-transfer mechanism. With this in mind, two octahedral nickel(II)/(III) complexes of a bis-tridentate N_2S donor carboxamide ligand, N-2-phenylthiophenyl-2′-pyridinecarboxamide (HL^{Ph}), have been synthesized, structurally characterized, and their SOD activities examined. These complexes mimic the full catalytic cycle of NiSOD. Electrochemical experiments support an outer-sphere electron-transfer mechanism for their SOD activity.*

The superoxide radical anions ($O_2^{\bullet-}$) that inevitably form as a by-product of aerobic metabolism can cause severe cellular damage in biological systems.[1] To combat such oxidative damage, living organisms have developed defense metalloenzymes, called superoxide dismutases (SODs),[2] that catalytically convert $O_2^{\bullet-}$ into O_2 and H_2O_2 by the reduction and oxidation of their redox-active metal centers, such as Fe, Mn, Ni, or Cu, in mononuclear FeSOD, MnSOD, NiSOD, and dinuclear Cu-ZnSOD, respectively, of which NiSOD was most recently identified. An analysis of the single-crystal X-ray structure of NiSOD revealed a square-planar $N_2S_2Ni^{II}$ reduced form and a square-pyramidal $N_3S_2Ni^{III}$ oxidized form as shown in Scheme 1.[3]

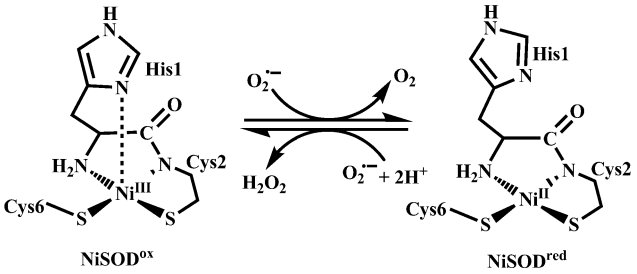

Scheme 1. Coordination geometry of oxidized (left) and reduced (right) forms of NiSOD active sites.

Efforts to synthesize nickel(II)/(III) complexes to structurally and/or functionally model NiSOD afforded several examples of such complexes with peptide-[4] and non-peptide-based[5] ligands. These reports account for important aspects of the structure–function relationship in NiSOD, such as the likely proton source for $O_2^{\bullet-}$ reduction to H_2O_2,[4b,k,5d–f] the role of "on" and "off" histidine-N (His-N) ligation axially to the nickel site,[4b,5b,h,i] and the rate of electron-transfer reactions.[4b,d,6] However, to understand the dismutation process, several key issues, as follows, require more intense study. 1) During dismutation, why does S-oxygenation of the cysteine-thiolato-sulfur residue not occur in an environment containing reactive oxygen species, such as $O_2^{\bullet-}$ and H_2O_2? Few models show S-oxygenation reactivity.[5b,c] 2) Does $O_2^{\bullet-}$ or O_2 interact with the Ni center either directly or indirectly through a secondary coordination sphere? Examples of Ni–dioxygen species are known.[7] 3) If no direct coordination to the Ni center occurs then is the Ni site required to have at least one vacant substrate binding site for its SOD activity? Biochemical evidence, both in favor[4e,f,h–k] and against[4b,5f,6] substrate binding to the nickel center, exists, in support of either an inner- or outer-sphere electron-transfer (ET) mechanism. Most of this evidence, including the low prevalence of S-oxygenation and very high rate (of an order of approximately 10^9) of catalytic $O_2^{\bullet-}$ disproportion, suggest an outer-sphere ET mechanism, although this is still somewhat ambiguous. Recent investigations support the binding of a CN^- moiety to the Ni center in a peptide-ligand environment, giving impetus to the ongoing debate.[4h] Indeed, the native NiSOD active site itself and all existing model complexes have one or more empty binding sites around the nickel center. Therefore, during dismutation the interaction of O_2, $O_2^{\bullet-}$, and H_2O_2 with the Ni center cannot be excluded. To resolve these questions regarding the mechanistic pathway of SOD activity, more functional models are required. Apart

[*] S. K. Chatterjee, R. C. Maji, Dr. A. K. Patra
Department of Chemistry
National Institute of Technology Durgapur
Mahatma Gandhi Avenue, Durgapur 713 209 (WB) (India)
E-mail: apurba.patra.nitdgp@gmail.com
S. K. Barman
Department of Chemistry, Indian Institute of Technology Kanpur
Kanpur 208 016 (India)
Prof. Dr. M. M. Olmstead
Department of Chemistry, University of California
Davis, CA 95616 (USA)

[**] A.K.P. acknowledges the DST, Govt. of India (Project number SR/S1/IC-35/2007) for financial support. S.K.C. and R.C.M. thank the CSIR and UGC, India, respectively, for Fellowships. The AvH Foundation (Germany) is acknowledged for an equipment donation grant for procuring a CHI 1120A spectroelectrochemical analyzer. We acknowledge Prof. R. Mukherjee, IIT Kanpur for providing various instrumental facilities.

Supporting information for this article is available on the WWW under http://dx.doi.org/10.1002/anie.201404133.

from a few examples of nickel–peptide derivatives (containing peptide ligands in which a sequence of 6–12 amino acids provide the same coordination environment about the Ni center as in native NiSOD),[4] there is only one definite example of a nickel(III) complex containing a non-peptide-based ligand (N_3O_2 donor).[5k] This complex can catalyze the oxidation of $O_2^{\bullet-}$ to O_2, one of the two half reactions, $M^{ox} + O_2^{\bullet-} \rightarrow M^{red} + O_2$, of the NiSOD catalytic cycle. No model complex of NiSOD with a non-peptide ligand has yet been shown to mimic the full catalytic cycle nor has been shown to demonstrate the outer-sphere ET mechanism for its SOD activity.

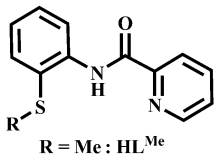

R = Me : HL^{Me}
R = Ph : HL^{Ph}

Scheme 2. Structural formula of ligands HL^R.

Herein, we report the first examples of nickel(II)/(III) complexes, $[(L^{Ph})_2Ni]$ (**1**) and $[(L^{Ph})_2Ni](ClO_4)\cdot H_2O$ (**2**·H_2O), which are derived from a tridentate monocarboxamide N_2S donor ligand, HL^{Ph} (Scheme 2, HL^{Ph} = N-2-phenylthiophenyl-2′-pyridinecarboxamide) that functionally mimic the full catalytic cycle of NiSOD. As the Ni center is hexacoordinated in these complexes with no vacant substrate binding site, the outer-sphere ET mechanism for their SOD activity is more likely.

In NiSOD, all of the nitrogen and sulfur donor atoms coordinated to the nickel center are of different types (one nitrogen each of amide, amine, and imidazole, one thiolate-sulfur atom, and one hydrogen-bonded thiolate-sulfur atom, which acts like a thioether sulfur). These donor atoms appear to tune the electron density surrounding the Ni center with the result that the $Ni^{II/III}$ redox couple is set to within the potential window of SOD activity. Recently, we reported that the amidato-N^- donor atom of the deprotonated HL^{Me} ligand (Scheme 2), as a result of its strong σ-donor ability, can stabilize significantly the higher oxidation state(s) of metal ions, such as copper(II) and nickel(III).[8] The relative stabilities of various Ni oxidation states (0, +1, +2, +3) and their correlation to both the hard/soft nature and the σ-donor/π-acceptor properties of the ligand donor center(s) has also been demonstrated.[8b] Although the coulometrically generated Ni^{III} species, $[(L^{Me})_2Ni]^+$, was observed, attempts to isolate it in pure form by using the chemical oxidant, $(NH_4)_2[Ce(NO_3)_6]$ (ammonium cerium(IV) nitrate, ACN) failed even at low temperature. As soon as $[(L^{Me})_2Ni]^+$ formed, it reverts back to its precursor quite quickly. Similar examples of the successful synthesis of pure Ni^{III} species by electrochemical methods rather than using a chemical oxidant have been established.[9] Herein, however, using the HL^{Ph} ligand we have been able to isolate pure **2** in good yield from its precursor **1** by using ACN as an oxidant, possibly resulting from the fine tuning of the thioether-sulfur donor ability, imposed by a phenyl substituent which had a ±R effect unlike the +I effect (R = resonance or mesomeric, I = inductive) of methyl group in the HL^{Me} ligand.

The Ni^{II} complex $[(L^{Ph})_2Ni]$ (**1**) was synthesized in dimethylformamide (DMF) by reaction of NaL^{Ph} with $[Ni(H_2O)_6](ClO_4)_2$ in a 2:1 molar ratio. In the FTIR spectrum of **1**, amide-nitrogen coordination to Ni^{II} is indicated by a change in the band of the carbonyl moiety, which undergoes a red shift ($\nu_{CO} = 1620\ cm^{-1}$) compared to $1680\ cm^{-1}$ for the free ligand. The magnetic moment of **1**, $\mu = 2.85$ B.M., measured by the Evans method in a solvent mixture of CH_2Cl_2 and C_6H_6, indicates that **1** is paramagnetic with two unpaired spins on the nickel(II) center ($S = 1$). The UV/Vis absorption spectrum of **1** measured in CH_3CN (with absorption bands λ_{max}/nm (ε/$M^{-1}\,cm^{-1}$) = 867 (66), 560 (25, shoulder), 340 (14880), 247 (28970) is comparable to those of other octahedral nickel(II) complexes.[8b] The single-crystal X-ray structure of **1**[10] revealed a distorted octahedral geometry about the Ni^{II} center. Two L^{Ph} ligands are bound to the Ni^{II} atom in a meridional fashion with two thioether-sulfur and two amidato-nitrogen donors of two ligands in *cis* and *trans* positions, respectively (Figure 1). The average Ni–N_{py}, Ni–N_{amide}, and Ni–S bond lengths of 2.0566(12) Å, 2.0258(11) Å,

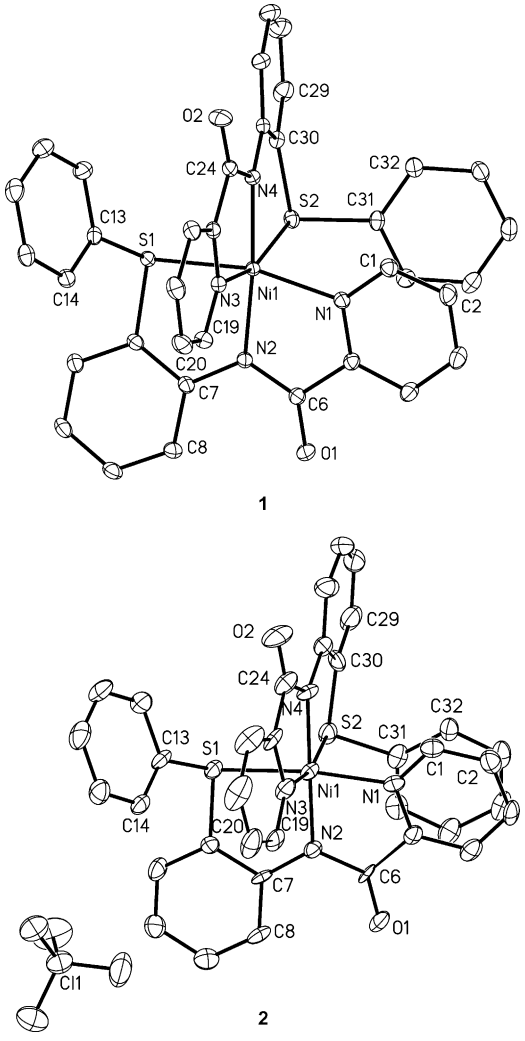

Figure 1. ORTEP diagrams of $[(L^{Ph})_2Ni]$ **1** (top) and $[(L^{Ph})_2Ni](ClO_4).H_2O$, **2**·$H_2O$ (bottom). Thermal ellipsoids are set at 50% probability and the H_2O molecule of **2** and H atoms are omitted for clarity. Selected bond lengths [Å] in $(L^{Ph})_2Ni$, **1** and [in $[(L^{Ph})_2Ni]^+$ ion of **2**]: Ni1-N1 2.0557(12) [1.993(5)], Ni1-N2 2.0182(11) [1.901(4)], Ni1-N3 2.0575(12) [2.025(5)], Ni1-N4 2.0334(11) [1.909(5)], Ni1-S1 2.4615(4) [2.3222(17)], Ni1-S2 2.4785(4) [2.3889(17)].

and 2.47(4) Å, respectively, are comparable to those of the complex $[(L^{Me})_2Ni]$, except for the Ni–S distance, which is approximately 0.026 Å longer in **1** (sulfur donor strength of -SPh is less than -SMe). The red-shifted UV/Vis absorption band at $\lambda = 867$ nm in **1** compared to $\lambda = 851$ nm for $[(L^{Me})_2Ni]$ clearly follow the similar trends, as previously observed[8b] for a weaker donor ligand. The cyclic voltammogram (CV) of **1** displays a reversible redox wave (see Figure S4 in the Supporting Information) which corresponds to the Ni^{II}/Ni^{III} couple at $E_{1/2} = +0.85$ V ($\Delta E_p = 60$ mV) versus SCE (SCE = saturated calomel electrode), a slightly more anodic potential than that of $[(L^{Me})_2Ni]$ as expected.

Addition of a CH_3CN solution of ACN to a yellow-colored solution of **1** in CH_2Cl_2 immediately generates a dark, reddish-brown solution from which **2** has been isolated in good yield. In the FTIR spectrum of **2**, a ν_{OH} band occurs at 3520 cm^{-1} and a ν_{CO} band at 1635 cm^{-1}. The ν_{CO} band is blue shifted compared to that of **1**, indicating coordination of the amidato-N^- atom to a nickel ion with an oxidation state greater than +2, that is, to Ni^{III}. The EPR spectrum of **2** in the solid state at room temperature displays an isotropic signal at $g = 2.09$ that in CH_2Cl_2 solution splits to form a five-line signal[8b,11] (a Ni^{III} spin coupled to the nuclear spin of two *trans* amide-nitrogen atoms). This signal has a super-hyperfine coupling constant, $A_{\parallel}^{N}$ (average), of 12 G (Figure S5) which confirms the presence of a Ni^{III} center and is further supported by its magnetic moment, $\mu = 1.69$ B.M ($S = 1/2$), corresponding to one unpaired spin. The UV/Vis absorption spectrum of **2** in CH_3CN (with absorption bands at λ_{max}/nm (ε/$M^{-1}cm^{-1}$) = 930 (120, shoulder), 775 (200), 445 (4500), 320 (17420), 250 (29500, shoulder)) is comparable to the reported Ni^{III} complexes with a N_4S_2 coordination sphere.[8b,9a,11c] Crystals suitable for X-ray diffraction were obtained by layering pentane on a CH_2Cl_2 solution of **2**. The ORTEP plot of the crystal structure of **2** is shown in Figure 1 (bottom). In general, the structure shows similar structural features to the nickel coordination environment in **1**, but has, however, shorter Ni–N and Ni–S bond lengths. The average $Ni–N_{py}$, $Ni–N_{amide}$, and Ni–S bond lengths of 2.009(6) Å, 1.905(5) Å, and 2.3554(19) Å, respectively, are approximately 0.05 Å, 0.12 Å, and 0.11 Å shorter than those of **1**, clearly indicating that the nickel center is in a +3 oxidation state in **2**. DFT calculations on **2** were performed using the Gaussian 09 program and considering X-ray structural coordinates without symmetry restrictions.[12] Results showed that the unpaired electron spin mainly resides on the Ni center with a Mulliken atomic spin density of +0.79 (Figure S6). To our knowledge, this is the first structural example of a Ni^{III} complex with amide-nitrogen and thioether-sulfur donors.

To investigate the capability of complexes **1** and **2** towards the dismutation of $O_2^{\bullet-}$ according to the following two half reactions of the NiSOD catalytic cycle [Eq. (1), (2)] and the concomitant shuttling between Ni^{II} and Ni^{III} oxidation states during the dismutation process, several experiments have been performed.

$$\mathbf{2} + O_2^{\bullet-} \rightarrow \mathbf{1} + O_2 \quad (1)$$

$$\mathbf{1} + 2H^+ + O_2^{\bullet-} \rightarrow \mathbf{2} + H_2O_2 \quad (2)$$

To investigate the SOD activity of **2**, a solution of **2** in CH_3CN (10^{-4} M) was titrated against a solution of KO_2 in CH_3OH (1 equiv KO_2 was dissolved in 100 μL CH_3OH, additions of this solution were then made in 10 μL aliquots). The progress of the reaction was monitored using UV/Vis absorption spectroscopy (Figure 2). With increasing additions

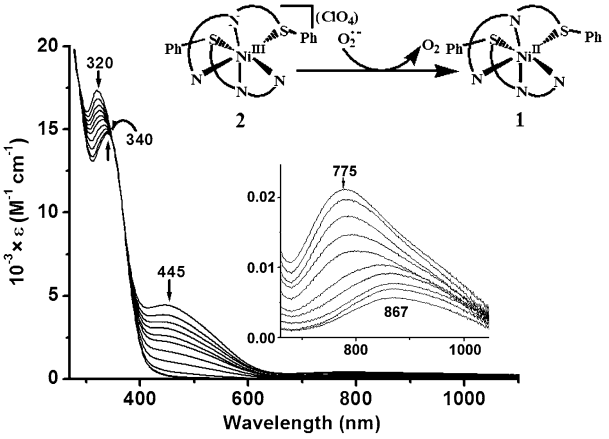

Figure 2. UV/Vis absorption spectra showing the conversion of a CH_3CN solution of **2** into **1** after the addition of CH_3OH solution of KO_2. Inset: Expanded portion of absorption spectrum ($\lambda = 650$–1050 nm).

of KO_2, the absorption band of **2** at $\lambda_{max} = 445$ nm vanishes and bands at $\lambda = 775$ nm and $\lambda = 320$ nm undergo red shifts to $\lambda = 867$ nm and $\lambda = 340$ nm, respectively. These bands correspond to the absorption bands evident in the spectrum of **1**. The isosbestic points at $\lambda = 365$ nm and $\lambda = 284$ nm indicate the clean transformation of **2** to form **1**. The molar extinction coefficients, ε, of the absorption bands at $\lambda = 340$ nm and $\lambda = 320$ nm are comparable to those of the independently synthesized complexes **1** and **2** respectively, confirming that the conversion of **2** into **1** is stoichiometric. This conversion is very fast and we believe that the reaction proceeds according to Equation (1). The release of O_2 gas is confirmed electrochemically (Figure S7, S8). In native NiSOD, the very high $O_2^{\bullet-}$ dismutation rate of the order of 10^9 strongly supports an outer-sphere ET mechanism for its SOD activity. To gain insight herein into the nature of ET processes, cyclic voltammetry experiments on **2** in the presence of KO_2 have been performed. Repeated scans of a solution of **2** in CH_3CN (10^{-3} M) after each addition of 20 μL of a total of 100 μL of a CH_3OH solution of stoichiometric KO_2, shown in Figure 3, revealed that the potential, current height, and ΔE_p values of the Ni^{II}/Ni^{III} couple were retained. These results strongly support that no structural reorganization during this Ni^{III} to Ni^{II} reduction process occurs and consequently confirms the outer-sphere ET from $O_2^{\bullet-}$ to a Ni^{III} metal center.

To examine the SOD activity of **1**, and to investigate whether the activity proceeds according to Equation (2), we have performed several experiments separately with KO_2 and $HClO_4$. First, it was found that the yellow solution of **1** in CH_3CN in the presence of KO_2 caused no change in the UV/Vis absorption spectrum with time. Second, when two equivalent of $HClO_4$ were added to a solution of **1** in

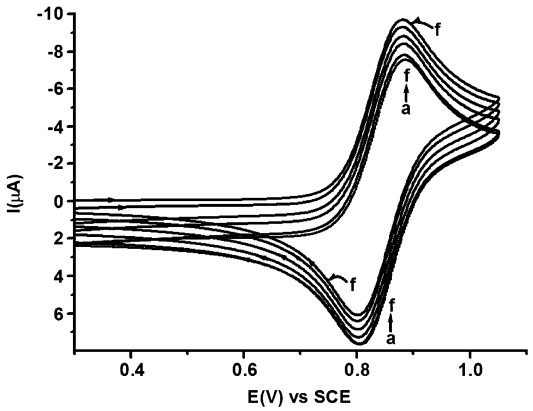

Figure 3. Cyclic voltammogram of **2** in CH_3CN (trace (a)) showing the conversion of **2** into **1** after the addition of a stoichiometric solution of KO_2 in CH_3OH (traces (b)→(f) after each addition of 20 μL of the KO_2 solution).

CH_3CN, complete loss of the ligand from the Ni^{II} center was observed (Figure S9). However, when the solution of **1** plus KO_2 is treated with $HClO_4$, the reaction then proceeds according to Equation (2). Next, we studied the SOD activity of **1** which was prepared by two different methods: a) in situ generated **1** from the reaction of **2** with KO_2 [Eq. (3)], and b) isolated solid **1**, synthesized from the reaction of NaL^{Ph} with $[Ni(H_2O)_6](ClO_4)_2$.

First, the SOD activity of in situ generated **1** was investigated. Stoichiometric production of **1** from a reaction of **2** with KO_2 [Eq. (3), step a] is evident from the UV/Vis absorption spectrum and the cyclic voltammogram as shown in Figures 2 and 3. **1** was treated with another equivalent of KO_2 followed by 2 equivalents of $HClO_4$ [Eq. (3), step b] after which the reddish brown color of **2** re-formed immediately. The formation of **2** was confirmed by the UV/Vis absorption spectrum and cyclic voltammetry (Figures S10, S11). An analysis of the UV/Vis absorption spectrum taken immediately after treatment with $HClO_4$ and focusing on the band at $\lambda = 445$ nm showed that approximately 75% of **2** was re-formed. The remaining 25% of **2** was converted back into **1** by reaction with produced H_2O_2 [Eq. (3), step c] following a similar reaction mechanism (proton-coupled ET reaction), as proposed by Solomon et al.[13] In this case, half an equivalent of O_2 with respect to complex **2** was formed from $HO_2^{\cdot}$ [Eq. (4)]. This formation of O_2 was confirmed electrochemically (Figure S12). In fact, following the proton-coupled ET reaction [Eq. (3), step c], the solution gradually faded within approximately five minutes from reddish-brown (resulting from generated **2**) to yellow (**1**).

$$\mathbf{2} + KO_2 \xrightarrow{a)} \mathbf{1} \xrightarrow[2\,HClO_4]{b)\,KO_2} \mathbf{2} + H_2O_2 \xrightarrow{c)} \mathbf{1} + HOO^{\cdot} + H^{+} \quad (3)$$

$$2\,HOO^{\cdot} \rightarrow O_2 + 2\,HO^{\cdot}\ (\text{or}\ H_2O_2) \quad (4)$$

The conversion of **2** into **1** using H_2O_2 as a reagent [Eq. (3), step c] has been confirmed in a separate experiment by using a solution of the isolated solid **2** in CH_3CN (Figure S13). Furthermore, the CV of the reaction mixture (composed of approximately 75% of **2** and 25% of **1**) taken immediately after treatment of **1** with $HClO_4$ and KO_2 [Eq. (3), step b] displays the same current height of the Ni^{III}/Ni^{II} couple as that of **1** before the addition of acid (Figure S11), indicating the conversion of generated **2** into **1** [Eq. (3), step c] and not to any other species. As both **1** and **2** display the same cyclic voltammogram, the total current height thus remain same, independent of the ratio of **1** to **2** present in the reaction mixture. The reversible conversion between **1** and **2** was also qualitatively investigated (through the appearance of the reddish brown/yellow color) through several cycles after the sequential addition of KO_2 and 2 equiv $HClO_4$. For this experiment, additional CH_3OH/CH_2Cl_2 was added to the reaction medium to prevent precipitation of **1** and KO_2 as they are highly soluble in this mixed solvent but not in pure CH_3CN.

Second, the SOD activity of isolated **1** was investigated. As compounds **1**, **2,** and KO_2 were shown to be highly soluble in CH_3OH/CH_2Cl_2 (1:1 v/v), the SOD activity of isolated **1** was examined in this mixed solvent medium. Additionally, CH_3OH helps to store protons by hydrogen bonding and supply it on demand in a controlled fashion to facilitate the transformation of **1** to **2** [Eq. (2)]. The solvent mixture was also suitable to monitor the formation of **2** by UV/Vis absorption spectroscopy (Figure 4). In fact, in this mixed

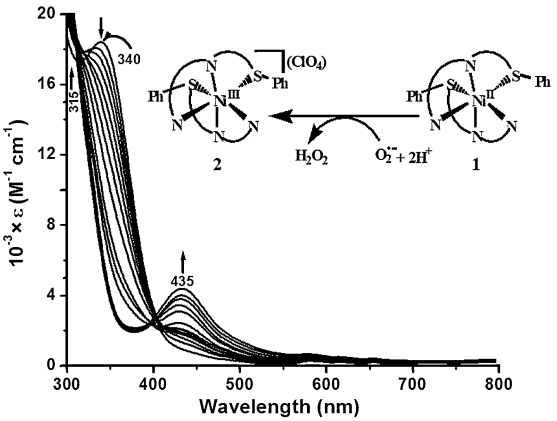

Figure 4. UV/Vis absorption spectra showing the conversion of a CH_3OH/CH_2Cl_2 (1:1 v/v) solution of **1** (10^{-4} M) + KO_2 → **2** after the addition of 6 equiv $HClO_4$ (200 μL) in CH_3OH solution. Each spectrum was recorded after the addition of 10 μL of the acid solution.

solvent, species **2** formed from the reaction of **1** plus KO_2 with $HClO_4$ is more stable even in the presence of generated H_2O_2, provided excess $HClO_4$ (6 equivalents to 1 equivalent of **1**) is used. It is likely that when excess acid is used, the formation of $HO_2^{\cdot}$ and H^+ from H_2O_2 is prevented [Eq. 3, step c], and therefore the generated **2** is more stable and is not converted back into **1** [Eq. (3), step c]. In contrast, in pure CH_3CN the reagent KO_2 is less soluble and so the added acid triggered de-metalation of the ligand (Figure S9) before complete transformation of **1** to **2** could occur. The formed **2** must react with H_2O_2 (if no excess acid is used) and re-form **1** by a proton-coupled ET reaction [Eq. (3), step c]. When a CH_3OH/CH_2Cl_2 solution of **1** plus KO_2 is treated with $HClO_4$ (6 equivalents), a reddish-brown color is generated

resulting from the formation of **2** (Figure 4). The new band at $\lambda_{max} = 435$ nm and the blue shift of the band at $\lambda = 340$ nm to $\lambda = 315$ nm correspond to those measured for **2** (same bands observed for isolated **2** in CH_3OH/CH_2Cl_2). Based on the extinction coefficient of the band at $\lambda = 435$ nm, the formation of **2** is stoichiometric (98%), although this reddish brown color gradually fades (2 h). The lack of clean isosbestic point(s) in Figure 4 unlike in Figure 2 is a result of the follow-up reaction of generated **2** with H_2O_2 and not with $HClO_4$ [Eq. (3), step c]. This step depends on the concentration of H^+ ions added, where a lower $[H^+]$ promotes the reaction of **2** with H_2O_2 but a greater $[H^+]$ suppresses it. Thus, the progressive addition of H^+ ions shifted the isosbestic points during the course of the experiment (Figure 4). Note, the solution of isolated **2** in CH_3OH/CH_2Cl_2 is stable in the presence of $HClO_4$, with no change evident in the UV/Vis absorption spectrum upon addition of up to 12 equivalents of $HClO_4$. The CV of the reddish brown solution generated displayed two redox couples, one at $E_{1/2} = -0.26$ V ($\Delta E_p =$ 90 mV), attributable to excess $HClO_4$ present in the reaction medium, and the other at $E_{1/2} = +0.84$ V which corresponds to the Ni^{II}/Ni^{III} couple of **2** (Figure S14). This CV clearly states that the generated **2** is stable in the presence of $HClO_4$ and H_2O_2 in this mixed solvent medium.

To understand the reason for the measured SOD activity of **1** and **2**, further cyclic voltammetry experiments were carried out. The CV of KO_2 in a solvent mixture of CH_3OH/CH_2Cl_2 (1:1 v/v) shows an irreversible wave which has $E_{pa} = +0.32$ V and $E_{pc} = -0.42$ V ($E_{pa} + E_{pc}/2 = -0.05$ V) for the $O_2^{\bullet-}/O_2$ couple. After addition of $HClO_4$ to this solution, the CV shows a new irreversible wave with $E_{pa} = +0.99$ V versus SCE for the $(HOO^{\bullet} + H^+)/H_2O_2$ couple (Figure S15). This wave corresponds to the proton-coupled reduction of $O_2^{\bullet-}$ to form H_2O_2 [$KO_2 + 2H^+ \rightarrow HO_2 + H^+ + K^+ \rightarrow H_2O_2^+ + K^+$; $H_2O_2^+ + e \rightarrow H_2O_2$]. These redox potentials of $O_2^{\bullet-}$ are very close to reported values of $+0.04$ V and $+1.03$ V versus Ag/AgCl respectively.[4a] The potential of $+0.99$ V for the $(HOO^{\bullet} + H^+)/H_2O_2$ couple is 110 mV more anodic than the $E_{pa} = +0.88$ V of the reversible Ni^{II}/Ni^{III} couple of **1**. Therefore, it should be possible to oxidize the $Ni^{II} \rightarrow Ni^{III}$, that is from **1** to **2**, and at the same time the species $HOO^{\bullet}$ and H^+, or $H_2O_2^+$ [Eq. (5)], will be reduced to H_2O_2 to complete the catalytic cycle.

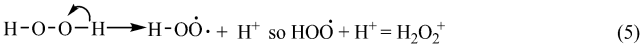

(5)

The CV of the yellow solution of **1** [Eq. (3), formed in step a] plus KO_2 displays the redox waves which correspond to the $O_2^{\bullet-}/O_2$ and Ni^{II}/Ni^{III} redox couples. However, when $HClO_4$ is added, inducing a color change from yellow to reddish brown, the $O_2^{\bullet-}/O_2$ couple vanishes and the response of the Ni^{II}/Ni^{III} couple remains unchanged with almost same current height and ΔE_p values (Figure S11). These results firmly establish the outer-sphere ET mechanism for this **1** to **2** conversion process [Eq. (2)]. Similarly, as $E_{1/2} = +0.85$ V of the Ni^{II}/Ni^{III} couple is more anodic than the $E_{pa} = +0.32$ V of the $O_2^{\bullet-}/O_2$ couple, the Ni^{III} complex, **2**, can easily oxidize $O_2^{\bullet-}$ to O_2 and will itself be reduced to form Ni^{II} complex **1** [Eq. (1)]. Interestingly, in the presence of weak acids, such as CH_3CO_2H and CF_3CO_2H, no formation of **2** is observed. Such weak acids are possibly unable to protonate $HO_2^{\bullet}$ to form the oxidant $H_2O_2^+$ and therefore are unable to oxidize Ni^{II} to Ni^{III}.

In summary, $[(L^{Ph})_2Ni]$ (**1**) and $[(L^{Ph})_2Ni](ClO_4)\cdot H_2O$ (**2**·H_2O) are the first examples of a set of NiSOD functional models with non-peptide ligands that mimic the full catalytic cycle of NiSOD. $[(L^{Ph})_2Ni](ClO_4)\cdot H_2O$ (**2**·H_2O) is the first example of a structurally characterized Ni^{III} complex with an amide-nitrogen and thioether-sulfur donor environment. These complexes are also the first examples of NiSOD functional models where the nickel center is hexacoordinated. Thus for the first time, direct support for an outer-sphere electron-transfer mechanism for SOD activity is obtained. The present work will provide a new route in the assessment of the mechanistic pathway of NiSOD activity.

Received: April 9, 2014
Revised: June 3, 2014
Published online: July 23, 2014

Keywords: electrochemistry · enzyme models · nickel · outer-sphere electron transfer · X-ray diffraction

[1] a) J. S. Valentine, D. L. Wertz, T. J. Lyons, L. L. Liou, J. J. Goto, E. B. Gralla, *Curr. Opin. Chem. Biol.* **1998**, *2*, 253 – 262; b) D. M. Kurtz, Jr., *Acc. Chem. Res.* **2004**, *37*, 902 – 908; c) J. A. Imlay, *Annu. Rev. Microbiol.* **2003**, *57*, 395 – 418; d) A. C. Maritim, R. A. Sanders, J. B. Watkins III, *J. Biochem. Mol. Toxicol.* **2003**, *17*, 24 – 38.

[2] a) A.-F. Miller, *Curr. Opin. Chem. Biol.* **2004**, *8*, 162 – 168; b) I. Fridovich, *Annu. Rev. Biochem.* **1995**, *64*, 97 – 112.

[3] a) E. P. Broering, P. T. Truong, E. M. Gale, T. C. Harrop, *Biochemistry* **2013**, *52*, 4 – 18; b) D. P. Barondeau, C. J. Kassmann, C. K. Bruns, J. A. Tainer, E. D. Getzoff, *Biochemistry* **2004**, *43*, 8038 – 8047; c) J. L. Wuerges, Y.-I. Yim, H.-S. Yim, S.-O. Kang, K. D. Carugo, *Proc. Natl. Acad. Sci. USA* **2004**, *101*, 8569 – 8574.

[4] a) J. Shearer, L. M. Long, *Inorg. Chem.* **2006**, *45*, 2358 – 2360; b) K. P. Neupane, K. Gearty, A. Francis, J. Shearer, *J. Am. Chem. Soc.* **2007**, *129*, 14605 – 14618; c) M. Schmidt, S. Zahn, M. Carella, O. Ohlenschläger, M. Görlach, E. Kothe, J. Weston, *ChemBioChem* **2008**, *9*, 2135 – 2146; d) J. Shearer, K. P. Neupane, P. E. Callan, *Inorg. Chem.* **2009**, *48*, 10560 – 10571; e) D. Tietze, H. Breitzke, D. Imhof, E. Kothe, J. Weston, G. Buntkowsky, *Chem. Eur. J.* **2009**, *15*, 517 – 523; f) D. Tietze, M. Tischler, S. Voigt, D. Imhof, O. Ohlenschläger, M. Görlach, G. Buntkowsky, *Chem. Eur. J.* **2010**, *16*, 7572 – 7578; g) M. E. Krause, A. M. Glass, T. A. Jackson, J. S. Laurence, *Inorg. Chem.* **2010**, *49*, 362 – 364; h) D. Tietze, S. Voigt, D. Mollenhauer, M. Tischler, D. Imhof, T. Gutmann, L. González, O. Ohlenschläger, H. Breitzke, M. Görlach, G. Buntkowsky, *Angew. Chem.* **2011**, *123*, 3002 – 3006; *Angew. Chem. Int. Ed.* **2011**, *50*, 2946 – 2950; i) M. E. Krause, A. M. Glass, T. A. Jackson, J. S. Laurence, *Inorg. Chem.* **2011**, *50*, 2479 – 2487; j) A. M. Glass, M. E. Krause, J. S. Laurence, T. A. Jackson, *Inorg. Chem.* **2012**, *51*, 10055 – 10063; k) J. Shearer, *Angew. Chem.* **2013**, *125*, 2629 – 2632; *Angew. Chem. Int. Ed.* **2013**, *52*, 2569 – 2572.

[5] a) J. Shearer, N. Zhao, *Inorg. Chem.* **2006**, *45*, 9637 – 9639; b) H. Ma, S. Chattopadhyay, J. L. Petersen, M. P. Jensen, *Inorg. Chem.* **2008**, *47*, 7966 – 7968; c) R. M. Jenkins, M. L. Singleton, E. Almaraz, J. H. Reibenspies, M. Y. Darensbourg, *Inorg. Chem.*

2009, *48*, 7280 – 7293; d) C. S. Mullins, C. A. Grapperhaus, B. C. Frye, L. H. Wood, A. J. Hay, R. M. Buchanan, M. S. Mashuta, *Inorg. Chem.* **2009**, *48*, 9974 – 9976; e) E. M. Gale, A. K. Patra, T. C. Harrop, *Inorg. Chem.* **2009**, *48*, 5620 – 5622; f) V. Mathrubootham, J. Thomas, R. Staples, J. McCraken, J. Shearer, E. L. Hegg, *Inorg. Chem.* **2010**, *49*, 5393 – 5406; g) E. M. Gale, B. S. Narendrapurapu, A. C. Simmonett, H. F. Schaefer III, T. C. Harrop, *Inorg. Chem.* **2010**, *49*, 7080 – 7096; h) D. Nakane, Y. Funahashi, T. Ozawa, H. Masuda, *Chem. Lett.* **2010**, *39*, 344 – 346; i) M. Gennari, M. Orio, J. Pécout, F. Neese, M.-N. Collomb, C. Duboc, *Inorg. Chem.* **2010**, *49*, 6399 – 6401; j) E. M. Gale, A. C. Simmonett, J. Telser, H. F. Schaefer III, T. C. Harrop, *Inorg. Chem.* **2011**, *50*, 9216 – 9218; k) E. M. Gale, D. M. Cowart, R. A. Scott, T. C. Harrop, *Inorg. Chem.* **2011**, *50*, 10460 – 10471; l) W.-Z. Lee, C.-W. Chiang, T.-H. Lin, T.-S. Kuo, *Chem. Eur. J.* **2012**, *18*, 50 – 53.

[6] S. B. Choudhury, J.-W. Lee, G. Davidson, Y.-I. Yim, K. Bose, M. L. Sharma, S.-O. Kang, D. E. Cabeli, M. J. Maroney, *Biochemistry* **1999**, *38*, 3744 – 3752.

[7] a) K. Shiren, S. Ogo, S. Fujinami, H. Hayashi, M. Suzuki, A. Uehara, Y. Watanabe, Y. Moro-oka, *J. Am. Chem. Soc.* **2000**, *122*, 254 – 262; b) D. Nakane, S. Kuwasako, M. Tsuge, M. Kubo, Y. Funahashi, T. Ozawa, T. Ogura, H. Masuda, *Chem. Commun.* **2010**, *46*, 2142 – 2144; c) J. Cho, H. Y. Kang, L. V. Liu, R. Sarangi, E. I. Solomon, W. Nam, *Chem. Sci.* **2013**, *4*, 1502 – 1508; d) M. T. Kieber-Emmons, C. G. Riordan, *Acc. Chem. Res.* **2007**, *40*, 618 – 625.

[8] a) R. C. Maji, S. K. Barman, S. Roy, S. K. Chatterjee, F. L. Bowles, M. M. Olmstead, A. K. Patra, *Inorg. Chem.* **2013**, *52*, 11084 – 11095; b) S. K. Chatterjee, S. Roy, S. K. Barman, R. C. Maji, M. M. Olmstead, A. K. Patra, *Inorg. Chem.* **2012**, *51*, 7625 – 7635.

[9] a) K. Pramanik, S. Karmakar, S. B. Choudhury, A. Chakravorty, *Inorg. Chem.* **1997**, *36*, 3562 – 3564; b) J. Hanss, H.-J. Krüger, *Angew. Chem.* **1998**, *110*, 366 – 369; *Angew. Chem. Int. Ed.* **1998**, *37*, 360 – 363.

[10] Diffraction data were collected on a Bruker Smart APEX II CCD area detector diffractometer at 90(2) K for **1** and at 120(2) K for **2**. Structures were solved by direct methods (*SHELXS*-97, Sheldrick, **2008**) and refined by using full-matrix least squares on F^2 (*SHELXL*, Sheldrick, **2013**) with all non-hydrogen atoms refined anisotropically. Crystal data for (**1**): Yellow block, monoclinic, space group $P2_1/n$, $a = 15.8112(13)$, $b = 13.0936(11)$, $c = 16.0002(13)$, $\beta = 116.8880(10)$, $V = 2954.3(4)$ Å^3, $Z = 4$, $\rho_{calcd} = 1.505$ Mg m^{-3}, $2\theta_{max} = 62.7°$, $F(000) = 1384$, $\lambda Mo_{k\alpha} = 0.71073$ Å, total reflections 9686, unique reflections 7926, parameters 406, $R1 = 0.0317$ and $wR2 = 0.0741$ for 7926 data ($I > 2\sigma(I)$). Crystal data for **2**: Purple block, monoclinic, space group $P2_1/c$, $a = 13.138(3)$, $b = 25.212(6)$, $c = 10.352(2)$, $\beta = 101.146(4)$, $V = 3364.3(13)$ Å^3, $Z = 4$, $\rho_{calcd} = 1.554$ Mg m^{-3}, $2\theta_{max} = 51°$, $F(000) = 1620$, $\lambda Mo_{k\alpha} = 0.71073$ Å, total reflections 6206, unique reflections 3478, parameters 468, $R1 = 0.063$ and $wR2 = 0.1491$ for 3478 data ($I > 2\sigma(I)$). CCDC-976750 (**1**), 977005 (**2**) contain the supplementary crystallographic data for this paper. These data can be obtained free of charge from The Cambridge Crystallographic Data Centre via www.ccdc.cam.ac.uk/data_request/cif.

[11] a) T. Storr, E. C. Wasinger, R. C. Pratt, T. D. P. Stack, *Angew. Chem.* **2007**, *119*, 5290 – 5293; *Angew. Chem. Int. Ed.* **2007**, *46*, 5198 – 5201; b) H.-J. Kruger, R. H. Holm, *J. Am. Chem. Soc.* **1990**, *112*, 2955 – 2963; c) A. K. Singh, R. Mukherjee, *Dalton Trans.* **2005**, 2886 – 2891.

[12] Gaussian 09 (Revision B.01), Frisch, et al., Gaussian, Inc.: Wallingford, CT, **2010**.

[13] R. K. Szilagyi, P. A. Bryngelson, M. J. Maroney, B. Hedman, K. O. Hodgson, E. I. Solomon, *J. Am. Chem. Soc.* **2004**, *126*, 3018 – 3019.

